GROWTH BEHAVIOR OF SHORT SURFACE FATIGUE CRACKS IN 2 1/4 Cr-1 Mo STEEL

Chang Min Suh*, Robert O. Ritchie** and Young Goo Kang***

Fatigue tests by axial loading ($R = 0.05$) were carried out to investigate short fatigue crack growth behavior in 2 1/4 Cr-1 Mo steel at room temperature using smooth and a small notched flat specimen. All the data of the fatigue crack growth rate in the present tests were analyzed as a function of the stress intensity factor equation in conjunction with crack closure behavior. Analysis was performed accounting for the relation of surface effective stress range, Ua and depth effective stress range, Ub. In the case of isotropic crack growth properties, $Ub = (\Delta K_{ia}/\Delta K_{ib}) \cdot Ua$. By use of Ub obtained from the analysis, crack growth rates to surface direction coincide with those of depth direction.

Key Words : Semi-Elliptical Crack, Surface Replica, Short Crack, Aspect Ratio, Beachmark Method, Effective Stress Range Ratio, Crack Opening Displacement.

1. INTRODUCTION

In recent years growing attention has been paid to short cracks (De Los Rios et al, 1984 ; Kitagawa et al, 1979 ; Suh, Kitagawa, 1987 ; El Haddad et al, 1979). Numerous investigations have been performed in an effort to characterize short crack behavior experimentally as well as analytically to understand mechanisms of early stage of fatigue cracks and fatigue processes associated with short cracks.

Although a considerable amount of investigation (Jono et al., 1985 ; Suh et al., 1984 ; Gangloff, 1981 ; Staal et al., 1979 ; Leis, 1985 ; Hudak, 1981 ; Iyyer and Dowing, 1986 ; Skelton, 1982) has been carried out thus far to clarify and to evaluate the growth behavior of short cracks, it is yet questionable whether the principal governing parameter for short cracks is identified. This may be attributed partly to the difficulties in experiment and analysis involved in studying short cracks.

Many attempts have been made to analyze short crack behavior by modifying the concept of LEFM. Several investigators have discovered the differences of fatigue growth behavior between long and short cracks (Kitagawa et al, 1979 ; El Haddad et al, 1979 ; Jono et al, 1985 ; Staal et al, 1979).

Accurate stress intensity factor solutions must be obtained to characterize short crack growth behavior by the concept of LEFM. Also, effective stress range ratios [Ua, Ub] for the points of intersection of the crack plane and the free surface and maximum crack penetration must be obtained to apply the concept of crack closure proposed by Elber in 1971. But the ratio of Ub is difficult to obtain from the experiment. Recently, it has been reported that the ratio of Ua/Ub becomes 0.91 for the elliptic surface flaw by the analytic method (Jolles et al., 1983).

In this paper, analysis of the fatigue growth of semi-elliptic surface crack was performed, and the value of Ub was estimated using Ua obtained from the experiment. Also, the growth and closure behaviors of short cracks initiated on the smooth and the notched specimens of 2 1/4 Cr-1 Mo steel were carefully examined and evaluated by the analytic method.

2. ANALYSIS OF SURFACE CARCK

2.1 Growth of Surface Crack

Consider the semi-elliptic surface crack in a finite plate as shown in Fig. 1. Dimension a is the half crack length along the plate surface, b is the crack depth, w is the plate thickness, and ϕ is the parametric angle defining a location on the crack border. Since observations of such cracks are that they remain essentially semi-elliptic (Suh et al., 1987), the growth of the surface crack can be studied by analyzing the growth
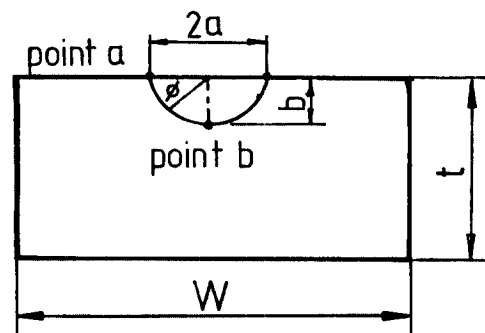
*Department of Mechanical Engineering, Kyung-pook National University, Taegu 702-701, Korea.
**Department of Materials Science and Mineral Engineering, University of CA, Berkeley, CA 94720, USA.
***Department of Mechanical Engineering, Kumho Institute of Technology, Kyung-pook, Kumi 730-070, Korea.

Fig. 1 Surface crack geometry

at the points of maximum crack penetration (point b) and intersection of the crack plance and free surface (point a). In the case of isotropic fatigue crack growth properties, the crack growth rates at these points can be related to the stress intensity factor range (ΔK_I) through the Paris equation in 1963 as Eq. (1) and Eq. (2),

$$da/dN = C[\Delta K_{Ia}]^n \tag{1}$$
$$db/dN = C[\Delta K_{Ib}]^n \tag{2}$$

where C and n can be shown now to be material constants.

2.2 Relation Between Ua and Ub

By use of the crack closure phenomenon, the crack growth rate equation can be written as Eq. (3) and Eq. (4),

$$da/dN = C[\Delta K_{Ia} \text{ eff.}]^m \tag{3}$$
$$db/dN = C[\Delta K_{Ib} \text{ eff.}]^m \tag{4}$$

where C and m are material constants. The extent of crack closure can be conveniently quantified by use of the effective stress range ratio as Eq. (5),

$$\frac{\sigma_{max.} - \sigma_{op.}}{\sigma_{max.} - \sigma_{min.}} = \frac{\Delta K_I \text{ eff.}}{\Delta K_I} \tag{5}$$

where $\sigma_{op.}$ is the crack opening stress level. The crack opening stress level at the intersection of a crack plane and a free surface can be determined experimentally from a plot of applied stress versus displacement across the crack faces. Then Eq.(5) can be used to determine the value of effective stress range ratio at point a, Ua.

Let the effective stress range ratio at point b be Ub.

$$Ua = \frac{\Delta K_{Ia} \text{ eff.}}{\Delta K_{Ia}} \tag{6}$$

$$Ub = \frac{\Delta K_{Ib} \text{ eff.}}{\Delta K_{Ib}} \tag{7}$$

Combining Eqs. (3), (4), (6) and (7) and writing in incremental form yields Eq. (8).

$$Ub = (\Delta b/\Delta a)^{\frac{1}{m}} \frac{\Delta K_{Ia}}{\Delta K_{Ib}} \cdot Ua \tag{8}$$

Here, let $(\Delta b/\Delta a)^{\frac{1}{m}} \fallingdotseq 1$, Then Eq. (8) can be written as Eq. (9).

$$Ub = (\Delta K_{Ia}/\Delta K_{Ib}) \cdot Ua \tag{9}$$

3. EXPERIMENTAL PROCEDURES

Axial tensile fatigue test of 2 1/4 Cr-1 Mo steel (A387) with short cracks initiated on smooth specimen and notched specimen was selected for this study.

The form of fatigue specimen (width of 14.5mm and thickness of 5mm) was a sandglass type. In case of notched specimen, a small artificial notch on the central portion of the specimen was drilled. The notch is circular, 0.5mm in diameter and 0.5mm in depth. The crack path was oriented in the transverse direction. The mechanical properties of the specimen are 435MPa for 0.2% yield stress, 508MPa for tensile strength, 27% for elongation ratio and 70% for reduction in

area. Fatigue testing was performed on a MTS electro-hydraulic closed loop testing system. Fatigue tests were conducted in ambient room air under tension-tension cycling of sinusoidal waveform. A cyclic frequency was 10 Hz and load ratio was $R = 0.05$

Successive observations and measurements were made on the surface at the central portion of the specimen throughout the fatigue test until final fracture was occurred. For these purposes, a combined surface replica and photomicrograph technique was applied. Before testing, the specimens were lightly electropolished in order to remove the light surface roughness induced by the metallographic polishing.

The amount of crack opening displacement (COD) of the short surface crack during one cycle, was measured by plastic replica method in five steps : $0.05\sigma_{max}, 0.25\sigma_{max}, 0.5\sigma_{max}, 0.75$ σ_{max} and σ_{max}. The variation of COD was measured on the photograph enlarged to a magnification of 2,000. The COD was obtained by measuring the distances between the distinctive marks across the surface crack length perpendicular to loading direction.

4. FATIGUE CRACK INITIATION AND GROWTH BEHAVIOR

Figure 2 shows the relationship between maximum tensile stress, σ max , and number of cycles to fracture, Nf, for the notched specimens and the unnotched smooth specimens in 2 1/4 Cr-1 Mo steel. In this figure, the number of load cycles for surface crack length 2 $a = 0.6$ mm ($\square$ marks), 2 $a = 1.0$ mm($\triangle$ marks) and for final fracture ($\bullet$ marks) of the notched specimens are shown. These three lines are almost parallel to one another. This is a very useful property for NDI and prediction of fatigue life. This result coincides with those of mild steels (Kitagawa et al, 1980 ; Suh et al, 1987) and stainless steel (Suh, Kim, 1984). Consequently, in the fatigue process of 2 1/4 Cr-1 Mo steel, surface cracks initiate before 10 to 20 percent of its fatigue life in general. Subsequent crack growth from smooth surface and notched surface to the failure of the specimens was monitored by using plastic replication techniques.

Figure 3(a) shows the variation of length for surface crack initiated at an artificial small notch, and Fig. 3(b) shows that at smooth specimen. Mark $\triangle$, $\bigcirc$ and $\square$ indicate a-N curves for 421 MPa, 441 MPa and 451 MPa of maximum tensile stress respectively. The data of crack depth in Fig. 3(a) were
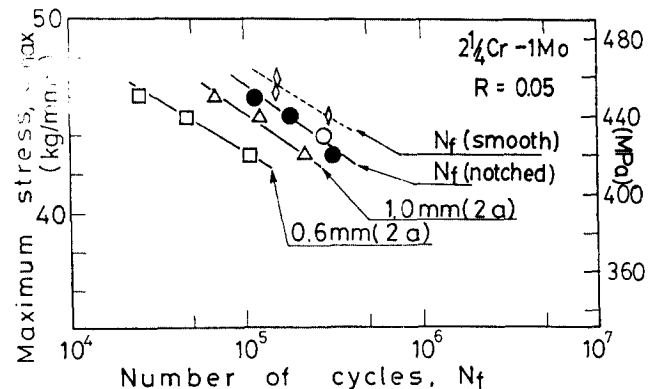

Fig. 2 The relationship between σ_{max}, and the number of cycles to fracture, Nf, and number of cycles to specified crack length
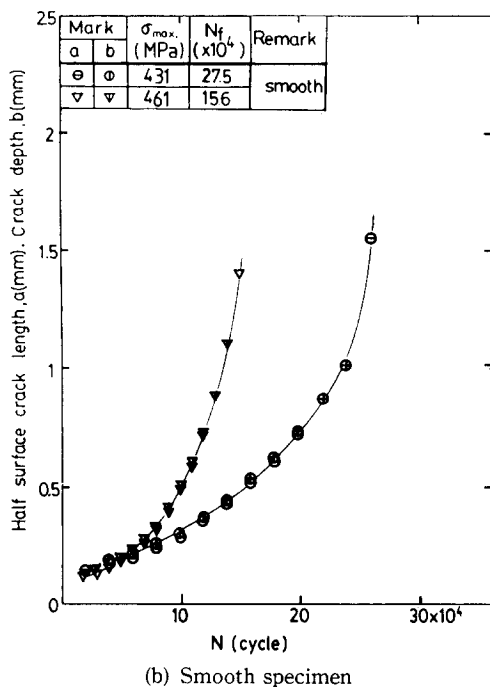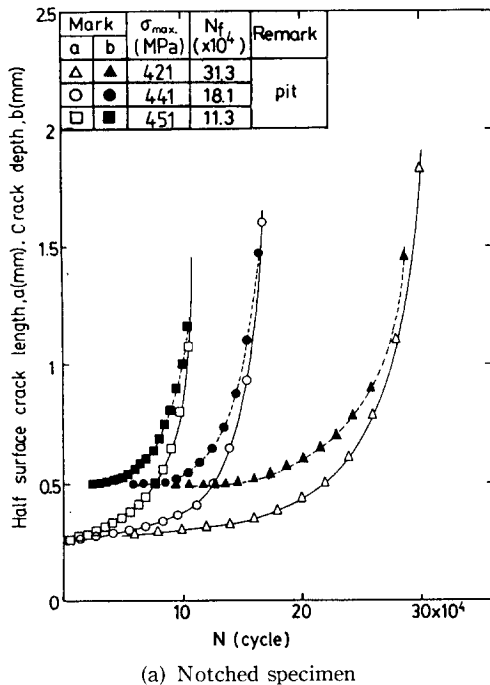
Mark		σ_{max}	N_f	Remark
a	b	(MPa)	($\times 10^4$)	
△	▲	421	31.3	
○	●	441	18.1	pit
□	■	451	11.3	

(a) Notched specimen

Mark		σ_{max}	N_f	Remark
a	b	(MPa)	($\times 10^4$)	
⊖	⦶	431	27.5	smooth
▽	▼	461	15.6	

(b) Smooth specimen

Fig. 3 Surface crack growth behavior

estimated by the aspect ratio of Fig. 4.

Marks▲, ● and ■ in Fig. 3(a) indicate b-N curves for 421 MPa, 441 MPa and 451 MPa of maximum tensile stress respectively. Marks ⦶ and ▽ of the smooth specimen in Fig. 3(b) indicate b-N curves for 431 MPa and 461 MPa of maximum tensile stress respectively. Two or three surface cracks were easily found at fractured surface of smooth specimen These cracks were initiated at inclusions or very small surface notches which can exist on the surface after electropolishing. The density of short surface crack is remarkably low compared to that of mild steels at room
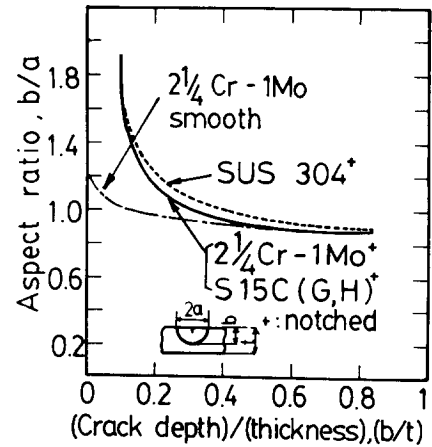

Fig. 4 Variation of aspect ratio

temperature (Kitagawa et al., 1980 ; Suh et al., 1987). This phenomenon was observed in type 304 stainless steel at room temperature (Suh and Kim, 1984).

Just before final fracture, some of the specimens were taken out of the test apparatus and temper colored for 1 hr. at 400°C. After final fracture of the specimens, the configurations of the cracks were observed and measured. A beach mark method was applied to obtain the aspect ratio of the surface cracks.

Figure 4 shows the variation of the aspect ratio that is the ratio of crack depth, b, to the half crack length, a, against the ratio of crack depth to the specimen thickness, t.

The aspect ratio of surface cracks in 2 1/4 Cr-1 Mo steel is similar to those of mild steels (Kitagawa et al, 1980 ; Suh et al., 1987) and stainless steel (Suh and Kim, 1984). The results of fatigue crack growth in Fig. 3 were further analyzed to obtain quantitative crack growth rate versus stress intensity factor data.

5. RELATIONSHIP OF CRACK LENGTH AND DEPTH TO CYCLE RATIO

The relationship between crack length and crack depth versus the cycle ratio is shown in Fig. 5. Fig. 5(a) and 5(b) is for the notched specimen, and Fig. 5(c) for the smooth specimen.

These figures show that :

(1) The short crack initiates and grows in the very early stage of fatigue life (e.g. 10-20% of life). Results presented in the recent literature (Suh and Kitagawa, 1987 : De Los Rios et al., 1984 ; El Haddad et al., 1979 ; Suh and Kim, 1984) agree well with this.

(2) The curve of the relationships between the crack length and cycle ratio are compressed into a relatively narrow band, regardless of stress level. This property is similar to that of mild steels (Suh and Kitagawa, 1987 ; Kitagawa et al., 1980 ; Suh et al., 1987) and stainless steels (Suh and Kim, 1984) as shown in Fig. 5(a) and 5(b).

(3) From (2), it can be suggested that an equi-crack length curve in Fig. 2 can be drawn almost in parallel to the S-Nf fracture curve.
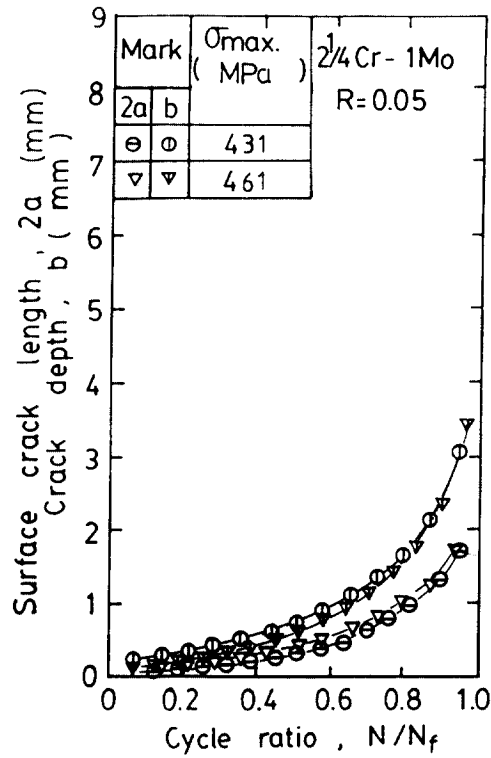
(4) Life prediction with respect to N/Nf, may be more practical and easier than that by the conventional procedures related to the residual life '(Suh and Kitagawa, 1987).
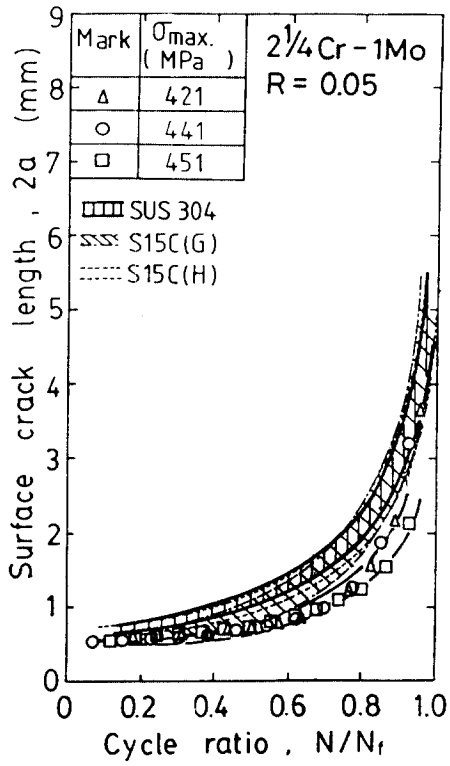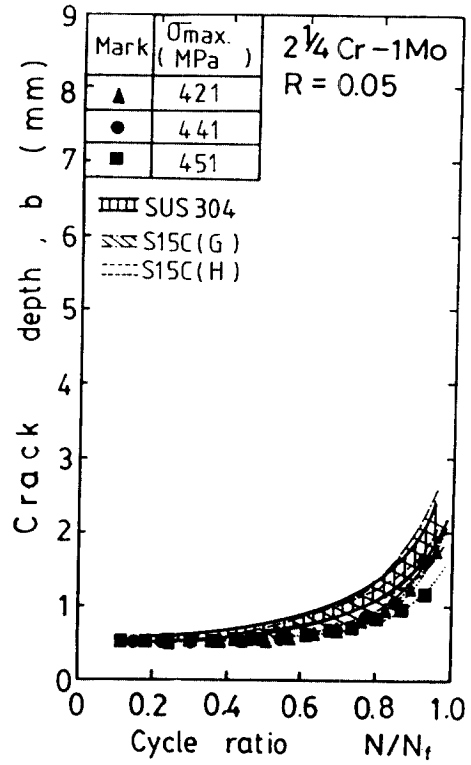
(a), (b) : Notched specimen (c) : Smooth specimen

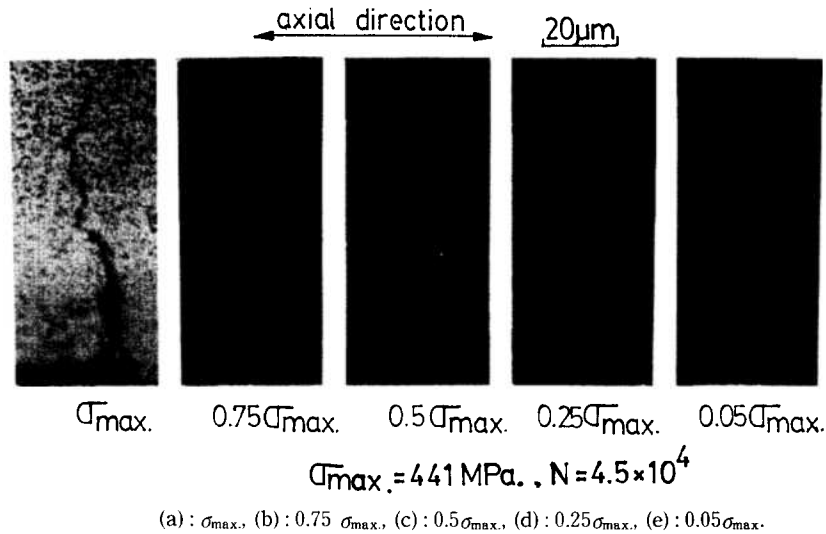**Fig. 5** Relationship between crack length and depth versus the cycle ratio

(a) : $\sigma_{max.}$, (b) : $0.75\,\sigma_{max.}$, (c) : $0.5\sigma_{max.}$, (d) : $0.25\sigma_{max.}$, (e) : $0.05\sigma_{max.}$.

Fig. 6 Photomicrographs of the crack tip during various stage of the cycle($\sigma_{max.}=441$MPa, $N=4.5\times10^4$)
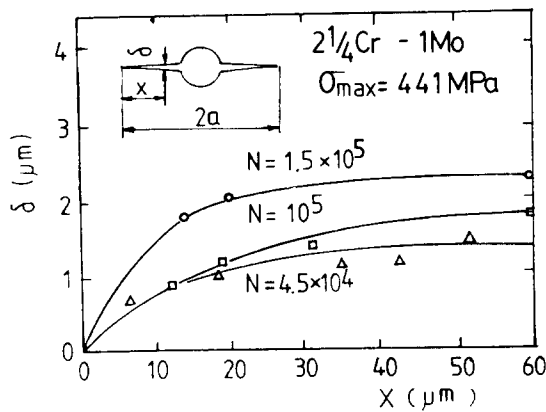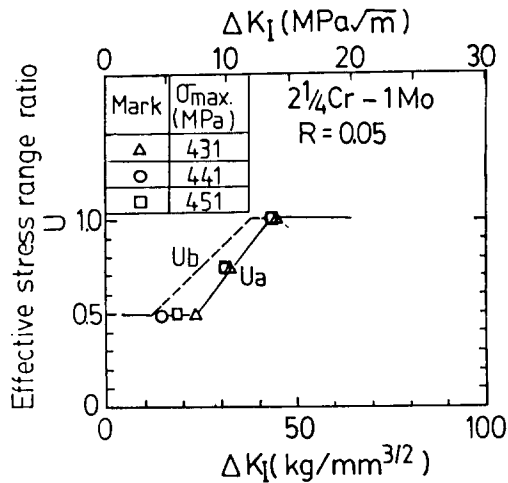

Fig. 7 Variations of COD along crack length

Fig. 8 Variations of effective stress range ratio U against stress intensity factor range ΔK_I
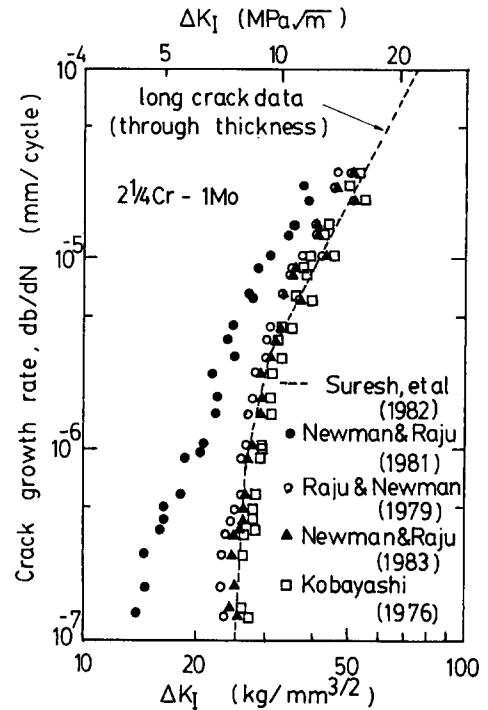

Fig. 9 Comparison of stress intensity factor range by four kinds of equation

6. CRACK OPENING DISPLACEMENT AND EFFECTIVE STRESS RANGE RATIO

The photographs of the crack tip region are presented in Fig. 6. The crack opening level appeared $0.5\sigma_{max}$ level. The variation of crack opening displacement (COD) along the crack tip is plotted in Fig. 7. Crack opening displacement

changed appreciably with crack length.

The variation of the effective stress range ratio, U_a (point a at Fig. 1) for short cracks is plotted against ΔK_l in Fig. 8, where the ratio U_a is calculated from eq. 5. As shown in Fig. 8, U_a increased with the growth of crack. This phenomenon is in agreement with the general conclusion of the reports (Staal, Elen, 1979 ; Ritchie, Yu, 1986) saying that U increases for increasing ΔK_l (and increasing R). On the other hand, the dependence of closure on crack length, indicated in this study as in Fig. 8, is in contradiction to the observation by other reports (Elber, 1971), saying that closure in Aluminum 2023-T3 shows practically no dependence on crack length.

7. COMPARISON OF STRESS INTENSITY FACTOR RANGE

Comparison of various calculation methods were carried out to find accurate solutions of stress intensity factor for surface cracks. Figure 9 shows the difference of stress intensity factor range depending on calculation method for the notched specimen of 2 1/4 Cr-1 Mo steel.

These figures shows that :

The ΔK_{lb} against the surface crack growth rate db/dN based on four different methods varied considerably. From these results the stress intensity factor range calculated by Newman and Raju's equations reported in 1983 are most closely approached to the data of through crack. Based on these results, the stress intensity factor range of this study were calculated by recently reported Newman and Raju's equations (1983).

$$K_{l}a = \Delta\sigma\sqrt{\pi b/Q} \ \ F \ (b/t, b/a, a/w, \phi) \tag{10}$$

where $\phi = \theta$

$$K_{l}b = \Delta\sigma\sqrt{\pi b/Q} \ \ F \ (b/t, b/a, a/w, \phi) \tag{11}$$

where $\phi = \pi/2$

8. GROWTH BEHAVIOR OF THE SURFACE CRACK

A functional relationship between crack growth rate and stress intensity factor was obtained independently of crack size and applied stress plotted in Fig. 10(a) for stress intensity values, ΔK_{lb}, based on Newman-Raju's equations (1983) respectively. Using the crack growth rate data for mild steel (Suh et al., 1987) and stainless steel (Suh and Kim, 1984), the stress intensity factor ranges were calculated by Newman and Raju equation. In Fig. 10(a) the results are also plotted as dotted lines and solid line respectively.

Figure 10(b) shows the crack growth rate, da/dN and db/dN, versus stress intensity factor range of smooth specimen. Figure 10(b) also shows the relation between smooth specimen data, scatter band of notched specimen data and solid line of long crack data on the same material. A little difference between the smooth specimen data and notched specimen data appears at low value of ΔK_l.

The crack growth rate of smooth specimen is faster than those of notched specimen and through crack. These similar
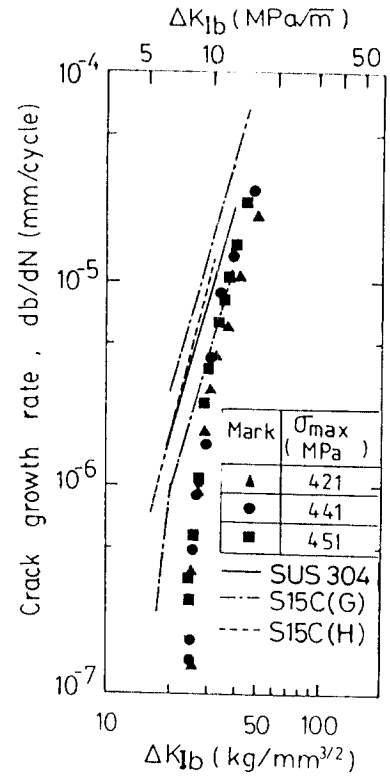
(a) Dependence of crack growth rate of crack depth upon the stress intensity factor range
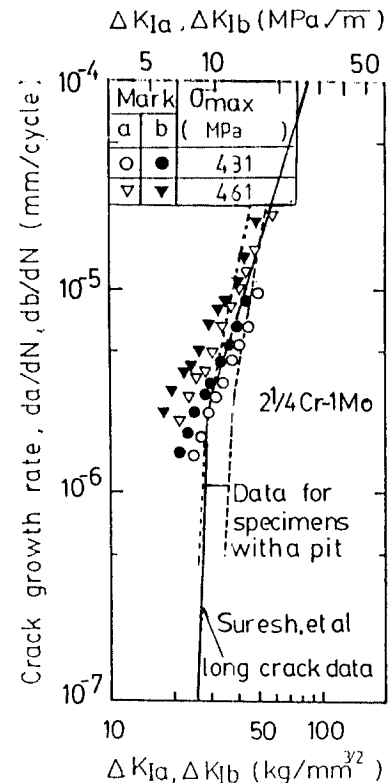
(b) Comparison of crack growth rate of smooth specimen notched specimen and large through crack
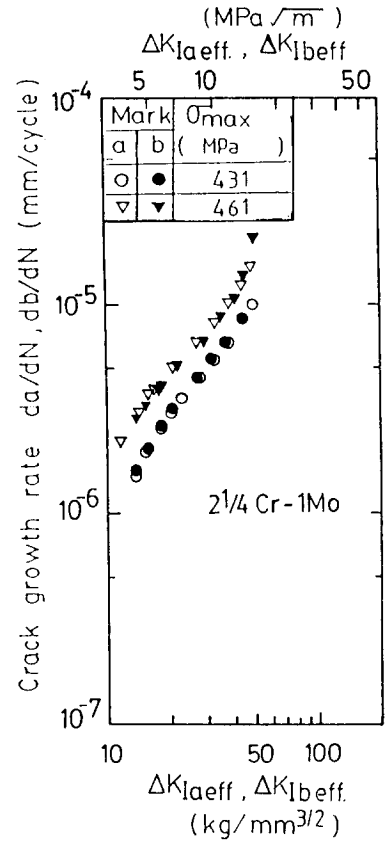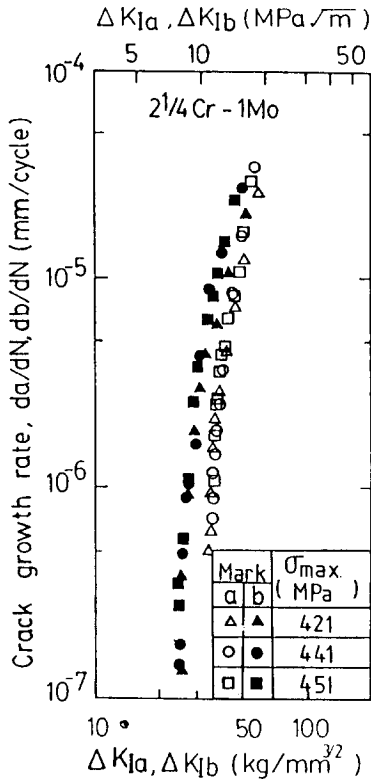
Fig. 10

Fig. 11 Dependence of the crack growth rate upon the effective stress intensity factor range for the notched specimen
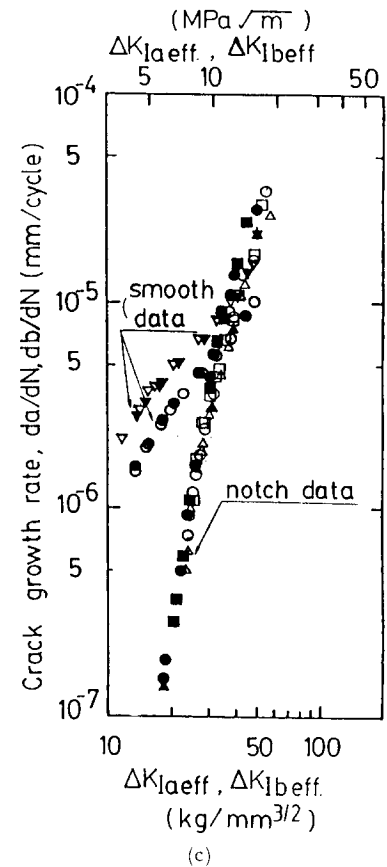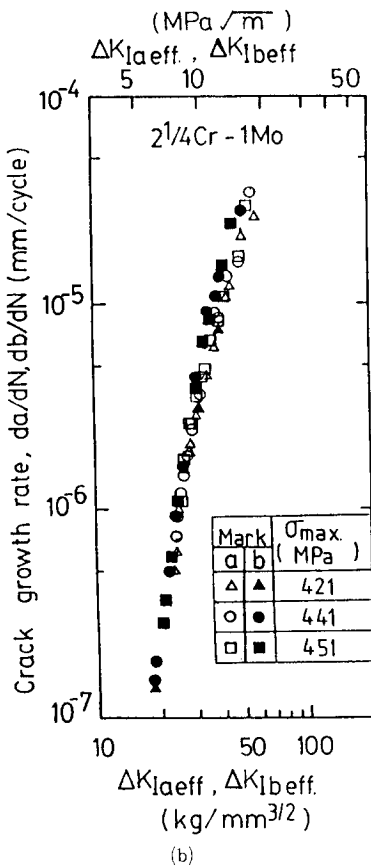

(a)

(b)

(c)

Fig. 12 Dependence of the crack growth rate upon the effective stress intensity factor range (a) smooth specimen (b) notched specimen (c) smooth and notched specimen

results were obained at other reports (Kitagawa et al., 1979 ; El Haddad et al., 1979 ; Hudak and Chan, 1986).

Figure 10(b) also shows the relation between crack growth rates $(da/dN, db/dN)$ and stress intensity factor ranges $(\Delta K_{ia}, \Delta K_{ib})$ for the smooth specimens of 2 1/4 Cr-1 Mo steel. For the notched specimens, it is shown in Fig. 11.

As shown in Fig. 10(b) and Fig. 11, crack growth rates at the point of maximum crack penetration (db/dN) are much faster than those of surface at the same value of ΔK_i. This difference in crack growth behavior caused by the difference of the extent of crack closure between the two points. Therefore, by use of the values of Ub obtained from Eq. (9) and Ua, the effective stress intensity factor ranges $(\Delta K_{ia}$ eff., ΔK_{ib} eff.) were estimated : this is plotted against da/dN, db/dN in Figs. 12(a), (b), (c). As shown in Figs. 12(a), (b), (c) crack growth rates of surface coincide with those of the point of maximum penetration for the two types of specimens of 2 1/4Cr-1 Mo steel.

9. RESULTS

Fatigue test by axial loading $(R = 0.05)$ were carried out to investigate short fatigue crack growth behavior in 2 1/4 Cr-1 Mo steel at room temperature using two types of specimens (smooth and notched flat specimen). In this paper, fatigue crack growth analysis was also carried out to examine the crack growth rate in conjuction with crack closure behavior. Analysis was performed accounting for the relation of effective stress ranges (Ua, Ub). The results are as follows :

(1) In the case of isotropic crack growth properties, the value of Ub can be approximated by

$$Ub = (\Delta K_{ia}/\Delta K_{ib}) \cdot Ua$$

(2) By use of Ub obtained from analysis, crack growth rate to surface direction coincides with those of depth direction.

(3) The crack growth rate of the smooth specimen is faster than that of notched specimen and large throught crack.

(4) The crack closure phenomenon appeared appeciably for low ΔK_i values and that of crack closure decreased for increasing ΔK_i.

(5) The density of small surface crack initiated on the smooth specimen is remarkably low, compared with that of mild steel.

REFERENCES

De Los Rios, E.R., Tang, Z. and Miller, K.J., 1984, "Short Crack Fatigue Behavior in a Medium Carbon Steel", Fatigue Fract. Engng. Mater. Struct. Vol. 7, pp. 97~108.

Elber, W., 1971, "The Significance of Fatigue Crack Closure", ASTM STP 486, pp. 230~242.

El Haddad, M.H., Smith, K.N. and Topper, T.H., 1979, "Fatigue Crack Propagation of Short Cracks", Trans. of ASME, J. of Engng. Mater. and Technology, No. 101, pp. 42~47.

Gangloff, R.P., 1981, "Quantitative Measurements of the Growth Kinetics of Small Fatigue Cracks in 10Ni Steel", ASTM STP 738, pp. 120~138.

Hudak, S.J.Jr., 1981, "Small Crack Behavior and the Prediction of Fatigue Life", J. of Eng. Materials and Technology, No. 103, pp. 26~35.

Hudak, S.J. Jr. and Chan, K.S., 1986, "In Search of a Driving Force to Charactering the Kinetics", Proc. of the 2nd Eng. Foundation Int. Conf. CA, pp. 379~405.

Iyyer, N.S. and Dowling, N.E., 1986, "Opening and Closing of Cracks at High Cyclic Strains", Proc. of the 2nd Eng. Foundation Int. Conf. CA, pp. 213~223.

Jolles M. and Tortoriello V., 1983, "Geometry Variations During Fatigue Growth of Surface Flaws", ASTM STP 791, pp. I-297~307.

Jono, M. and Song,J., 1985, "Growth and Closure of Short Fatigue Cracks", Material Research series, Vol. 1, pp. 35~55.

Kitagawa, H., Takahashi, S., Suh, C.M. and Miyashita S., 1979, "Quantitative Analysis of Fatigue Process-Microcracks and Slip Lines under Cyclic Strains", ASTM STP 675, pp. 420~449.

Kitagawa, H., Yuuki, R. and Suh, C.M., 1980, "Growth Behaviors of Fatigue Surface Crack initiated at a Small Artificial Notch", Preprint of Soc. of Mater. Science Japan, pp. 26~30.

Leis, B.N., 1985, "Displacement Controlled Fatigue Crack Growh in Inelastic Notch Fields : Implications for Short Cracks", Engineering Frac. Mechanics, Vol. 22-2, pp. 279~293.

Paris, P.C. and Erdogan F., 1963, "A Critical Analysis of Crack Propagation Law", ASME J. of Basic Eng. 85, pp. 528~538.

Raju, I.S. and Newman, J.C. Jr., 1979, "Stress Intensity Factors for a Wide Range of Semi-elliptical Surface Cracks in Finite-Thickness Plates", Engineering Fracture Mechanics, Vol. 11-4, pp. 817~829.

Newman, J.C.Jr., and Raju, I.S., 1983, "Stress Intensity Factor Equations for Cracks in Three-Dimensional Finite Bodies", ASTM STP 791, pp. I-238~265.

Newmann, J.C.Jr., and Raju, I.S., 1981, "An Empirical Stress Intensity Factor Equation for the Surface Crack", Engineering Fracture Mechanics, Vol. 15-1, pp. 185~192.

Ritchie, R.O. and Yu, W., 1986, "Short Crack Effects in Fatigue : A Consequence of Crack Tip Shielding", Proc. of the 2nd Eng. Foundation Int. Conf. CA, pp. 167~189.

Skelton, R.P., 1982, "Growth of Short Cracks During High Strain Fatigue and Thermal Cycling", ASTM STP 770, pp 337~381.

Staal, H.U. and Elen, J.D., 1979, "Crack Closure and Influence of Cycle Ratio R on Fatigue Crack Growth in Type 304 Stainless Steel at Room Temperature", Eng. Fracture Mechanics, Vol. 11, pp. 275~283.

Suh, C.M. and Kim, G.N., 1984, "A Study on the Initiation and Growth Behaviors of Surface Crack in Type 304 Stainless Steel at Room Temperature", Trans. of KSME, Vol. 8, pp. 195~200.

Suh, C.M. and Kitagawa, H., 1987, "Crack Growth Behaviour of Fatigue Microcracks in Low Carbon Steels", Fatigue Fract. Engng. Mater, Struct. Vol. 9, pp. 409~424.

Suh, C.M., Kwon, O.H. and Lee J.J., 1987, "Crack Growth Behavior of Fatigue Surface Crack Initiated from a Small Surface Defect", Trans. of KSME, Vol. 11, pp. 191~197.

Suresh, S., Zamiski, G.F. and Ritchie, R.O., 1982, "Fatigue Crack Propagation Beavior of 2 1/4Cr-1 Mo Steels for Thick-Wall Pressure Vessels", ASTM STP 755, pp. 49~67.